Control of Active Mobile Substations Under System Faults

Nima Yousefpoor, Ali Azidehak, Subhashish Bhattacharya
ECE Department
North Carolina State University
Raleigh, NC, USA
{nyousef, aazideh, sbhattacharya}@ncsu.edu

Babak Parkhideh
Energy Production and Infrastructure Center
ECE Department
UNC-Charlotte
Charlotte, NC, USA
bparkhideh@uncc.edu

***Abstract*— While conventional mobile substations are used to bypass the whole substation in case of loss or maintenance of power transformers, Active Mobile Substations (AMS) can be used both in normal conditions as a power router and in contingencies as a recovery transformer. The AMS is a mobile substation with integrated power electronics. By controlling its throughput power, it can be connected across different transformers of the grid. This paper explores transmission-level active mobile substations that provide back-up in case of power transformer failure or forced reduced operation scenarios in addition to power flow control for seasonal renewable energy transmission. The AMS must be designed to operate satisfactorily under typical fault and unbalanced conditions. In this paper, component design considerations in development of the AMS under unbalanced operating condition will be provided, and a new control strategy is proposed to control AMS under unbalanced operating conditions when component design is not sufficient to prevent overcurrent and trips. Detailed PSCAD simulation for the proposed control scheme is performed and results are presented. Experimental results are also shown to verify the proposed control method under unbalanced operating conditions.**

***Index Terms*-- Active Mobile Substation, Recovery Transformer, Disaster Management, Angle Control, System Fault, Instantaneous Active power Method, Component Design.**

I. INTRODUCTION

Mobile transformers/substations are commercially available, and "Polytransformer" from ABB-Spain with multi-voltage windings is considered as the current state-of-the-art technology which was introduced in 2005 [1]. Polytransformer's main application is universal spare and it is a practical approach that adds values to conventional mobile transformers due its flexibility of use for different transmission voltage levels up to 400kV. The voltage rating is selected by changing connections internally prior to moving the transformer to a new location. Compactness of the design comes with auto-transformer structure and magnetic core enclosing the windings and horizontal lay-down operation to match the transportation and hauling restrictions. Reinstallation of the polytransformer is expected to be about 15 days within the utility.

Conventional mobile substations are used to bypass the whole substation in case of a loss or maintenance of power transformers. The proposed transmission active mobile substation (AMS) in [2] can be also utilized in normal power systems conditions to extend the life-time of aging power transformers in the US. The AMS can regulate the throughput power of the main transformer by monitoring the transformer/substation's loading level, harmonic levels and impedance with disturbance signatures [3]. Therefore, AMS provides multi-functionality compared to conventional mobile substations.

With the development of the proposed AMS, transmission owners and system operators will possess a transportable, controllable, and versatile *asset* that helps them to restore power in case of natural disasters and emergencies. Utilities can also deploy or rent AMS to extend the life-time of their transformer fleet or (and with some provisions) to control the power flow from integration of renewable resources. Furthermore, future transmission substations can be envisioned with the developed AMS technology.

In order to meet the technical and economic targets, there are a number of fundamental design issues regarding flexible compact design of the power electronics converters (and power devices), fault tolerance of the converter system and operation under power system disturbances, insulation coordination, increased power density, cooling, system level control and communications that will need to be addressed to realize all aspects of the AMS.

In this paper, dynamic performance of AMS under unbalanced operating conditions is explored. Component design is performed such that negative sequence current is minimized under typical unbalanced conditions. A new control scheme is also proposed to control AMS under fault operating conditions. The angle control structure is employed to control the converter under normal operating conditions, and the supervisory control will switch the control structure from angle control method to the proposed control method when component design cannot mitigate the negative sequence current component of the converter appropriately when fault happens. The proposed control method is based on instantaneous active power control method. Detailed dynamic performance analysis of the AMS based on the angle control and proposed control method is presented. Experimental

results are also shown to evaluate the dynamic performance of angle-controller AMS under normal and unbalanced operating conditions.

This paper is organized as follows. In section II, power electronic building block of the proposed AMS is briefly explored. Section III provides component design of AMS for unbalanced operating conditions. The control structure of AMS based on instantaneous active power control method is proposed in section IV. Section V describes the hardware prototype of AMS. Experimental results are also presented to verify the angle-controlled AMS under normal and unbalanced operating conditions. Finally, Section VI draws the conclusions of this research work.

II. Power Electronic System Components of Active Mobile Substations

The building block for power electronic system of the proposed active mobile substation is a group of standard three phase drive converters presented in Fig. 1. In this figure, 24-pulse operation of the converters has been presented for two BTB converters. It is important to mention that *dynamic* and *steady-state* 24-pulse operation is obtained through the "angle-control" while with common vector-control methods (often known as PWM) for Voltage-sourced converters (VSCs) 12-pulse operation is attained [4]. To have complete angle control solution, i.e. BTB operation with superior THD, efficiency, and converter utilization indexes, advanced angle control structure proposed in [5] is used to accommodate the active power transfer as well as reactive power control. While the proposed angle-controlled configuration benefits from the occupied space and cooling requirements, being necessary for mobile substations, the operation of the system depends significantly on the passive components unlike the PWM converters as explained in [2].

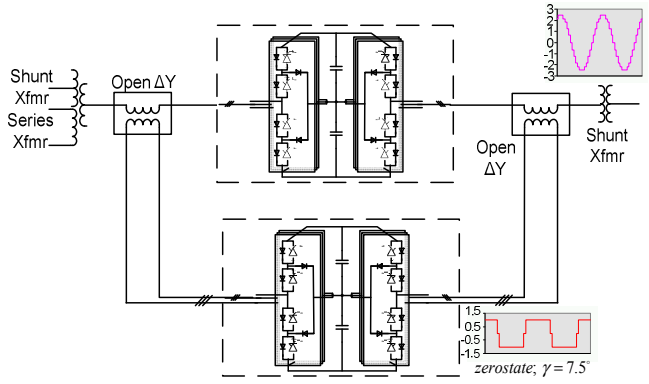

Fig. 1. Configuration of the power electronic system for the proposed active mobile substation.

III. Proposed Component Design Of AMS For Unbalanced Operating Conditions

The general schematic of a three phase AMS circuit is shown in Fig. 2. The negative sequence harmonic currents of AMS can be obtained by inserting a harmonic voltage source in series with the input voltage source. If we ignore losses ($R=0$), the state space equations of angle-controlled AMS in the dq synchronous reference frame can be written as (1). α_1 and α_2 are considered as two input variables to control VSC1 and VSC2. (1) can be linearized around steady state equilibrium points as can be expressed by (2).

The linearized state space equations of angle-controlled AMS under unbalanced operating conditions can be expressed as (3) steady state conditions ($\alpha_{10}=\alpha_{20}$) where $V_1 cos(2wt)$ and $V_1 sin(2wt)$ represents the dq components of the negative sequence voltage vector [3]. (3) is solved to calculate the dq components of the input currents as can be seen in (4)~(7). (8) also presents an algebraic equation for dc bus voltage. The magnitude of negative sequence current is also expressed by (9) when $V_{1=} V_{2=} V_{-1}$, and the magnitude of second order harmonic components of dc bus voltage is also presented by (10).

Fig. 3 shows negative sequence current component versus dc link capacitor value based on (9), and the second order harmonic component of dc bus voltage with respect to dc link capacitor is shown in Fig. 4.

The AMS must be designed to operate satisfactorily under typical fault and unbalanced conditions. Therefore, under unbalanced conditions due to presence of negative sequence voltage, an undesired current can flow into the system. This current can be high enough to shut down the whole AMS in order to avoid saturation of the interfacing transformers and over-heating of the switches. It is worth mentioning that producing direct positive and negative sequence voltages seen in PWM or vector-controlled converters is not possible in angle-controlled converters. Therefore, we designed the system and the capacitor such that (100)120 Hz oscillations in the DC link can be tolerated under typical unbalanced conditions. The 120 Hz oscillations in the DC link can produce appropriate negative sequence voltage in control and modulation structures and consequently minimize the negative sequence current. The dynamic performance of the AMS system with 1mF and 0.1 mF DC link capacitors under an unbalanced condition is simulated in PSCAD, and the results are presented in Figs. 5, and 6 respectively. The unbalanced system is represented by 50% voltage drop in phase-A of the inverter and rectifier side. As can be observed, the negative sequence current with higher amount of capacitance is higher. With higher active and reactive power demand, the generated negative sequence can be much higher as expected. Under the same condition, the negative sequence current flowing through the system versus the DC link capacitor value is also measured and the result is shown in Fig. 7. As can be seen, the negative sequence current is highly dependent on the DC capacitor value. Starting from very low values of capacitance, this current can be very low. It increases as the capacitor value increases until the system can be completely unstable due to the fact that the second harmonic of the line frequency is equal to the AMS resonant-pole frequency. Moving away from the resonant frequency brings the converter into the stable operation region. However, a huge capacitor is needed to achieve the desirable performance.

$$p\begin{bmatrix} i_{d1} \\ i_{q1} \\ V_{dc} \\ i_{d2} \\ i_{q2} \end{bmatrix}=\begin{bmatrix} 0 & \omega & \frac{k\omega}{L}\cos(\alpha_1) & 0 & 0 \\ -\omega & 0 & \frac{k\omega}{L}\sin(\alpha_1) & 0 & 0 \\ -\frac{3}{2C}k\omega\cos(\alpha_1) & -\frac{3}{2C}k\omega\sin(\alpha_1) & 0 & -\frac{3}{2C}k\omega\cos(\alpha_2) & -\frac{3}{2C}k\omega\sin(\alpha_2) \\ 0 & 0 & \frac{k\omega}{L}\cos(\alpha_2) & 0 & \omega \\ 0 & 0 & \frac{k\omega}{L}\sin(\alpha_2) & -\omega & 0 \end{bmatrix}\begin{bmatrix} i_{d1} \\ i_{q1} \\ V_{dc} \\ i_{d2} \\ i_{q2} \end{bmatrix}-\frac{\omega}{L}\begin{bmatrix} V_{d1} \\ V_{q1} \\ 0 \\ V_{d2} \\ V_{q2} \end{bmatrix} \tag{1}$$

$$p\begin{bmatrix} \Delta i_{d1} \\ \Delta i_{q1} \\ \Delta V_{dc} \\ \Delta i_{d2} \\ \Delta i_{q2} \end{bmatrix}=\begin{bmatrix} 0 & \omega & \frac{k\omega}{L}\cos(\alpha_{10}) & 0 & 0 \\ -\omega & 0 & \frac{k\omega}{L}\sin(\alpha_{10}) & 0 & 0 \\ -\frac{3}{2C}k\omega\cos(\alpha_{10}) & -\frac{3}{2C}k\omega\sin(\alpha_{10}) & 0 & -\frac{3}{2C}k\omega\cos(\alpha_{20}) & -\frac{3}{2C}k\omega\sin(\alpha_{20}) \\ 0 & 0 & \frac{k\omega}{L}\cos(\alpha_{20}) & 0 & \omega \\ 0 & 0 & \frac{k\omega}{L}\sin(\alpha_{20}) & -\omega & 0 \end{bmatrix}\begin{bmatrix} \Delta i_{d1} \\ \Delta i_{q1} \\ \Delta V_{dc} \\ \Delta i_{d2} \\ \Delta i_{q2} \end{bmatrix}-\frac{\omega}{L}\begin{bmatrix} \Delta V_{d1} \\ \Delta V_{q1} \\ 0 \\ \Delta V_{d2} \\ \Delta V_{q2} \end{bmatrix}+\begin{bmatrix} B_\alpha \end{bmatrix}\begin{bmatrix} \Delta\alpha_1 \\ \Delta\alpha_2 \end{bmatrix} \tag{2}$$

$$p\begin{bmatrix} i_{d1} \\ i_{q1} \\ V_{dc} \\ i_{d2} \\ i_{q2} \end{bmatrix}=\begin{bmatrix} 0 & \omega & \frac{k\omega}{L} & 0 & 0 \\ -\omega & 0 & 0 & 0 & 0 \\ -\frac{3}{2C}k\omega & 0 & 0 & -\frac{3}{2C}k\omega & 0 \\ 0 & 0 & \frac{k\omega}{L} & 0 & \omega \\ 0 & 0 & 0 & -\omega & 0 \end{bmatrix}\begin{bmatrix} i_{d1} \\ i_{q1} \\ V_{dc} \\ i_{d2} \\ i_{q2} \end{bmatrix}-\frac{\omega}{L}\begin{bmatrix} V+V_1\cos(2\omega t) \\ -V_1\sin(2\omega t) \\ 0 \\ V+V_2\cos(2\omega t) \\ -V_2\sin(2\omega t) \end{bmatrix} \tag{3}$$

$$i_{d1}(t)=\frac{(V_1-V_2)}{2L}\sin(\omega t)-\frac{(2LV_1C-V_1k^2+V_2k^2)}{2L(LC-k^2)}\sin(2\omega t)+\frac{\sqrt{C}(LV_1C-2LVC+LV_2C+2Vk^2+V_1k^2+V_2k^2)}{2\sqrt{L}(LC-k^2)\sqrt{(3k^2+LC)}}\sin(\frac{\sqrt{(3k^2+LC)}}{\sqrt{LC}}\omega t) \tag{4}$$

$$i_{q1}(t)=\frac{(4LVC+3V_1k^2+3V_2k^2)}{4L(LC+3k^2)}+\frac{(V_1-V_2)}{2L}\cos(\omega t)-\frac{(4LV_1C-3V_1k^2+V_2k^2)}{4L(LC-k^2)}\cos(2\omega t)+\frac{(LV_1C-2LVC+LV_2C+2Vk^2+V_1k^2+V_2k^2)}{2\sqrt{L}(LC-k^2)\sqrt{(3k^2+LC)}}\cos(\frac{\sqrt{(3k^2+LC)}}{\sqrt{LC}}\omega t) \tag{5}$$

$$i_{d2}(t)=\frac{(V_2-V_1)}{2L}\sin(\omega t)-\frac{(2LV_2C-V_2k^2+V_1k^2)}{2L(LC-k^2)}\sin(2\omega t)+\frac{\sqrt{C}(LV_2C-2LVC+LV_1C+2Vk^2+V_2k^2+V_1k^2)}{2\sqrt{L}(LC-k^2)\sqrt{(3k^2+LC)}}\sin(\frac{\sqrt{(3k^2+LC)}}{\sqrt{LC}}\omega t) \tag{6}$$

$$i_{q2}(t)=\frac{(4LVC+3V_1k^2+3V_2k^2)}{4L(LC+3k^2)}+\frac{(V_2-V_1)}{2L}\cos(\omega t)-\frac{(4LV_2C-3V_2k^2+V_1k^2)}{4L(LC-k^2)}\cos(2\omega t)+\frac{(LV_1C-2LVC+LV_2C+2Vk^2+V_1k^2+V_2k^2)}{2\sqrt{L}(LC-k^2)\sqrt{(3k^2+LC)}}\cos(\frac{\sqrt{(3k^2+LC)}}{\sqrt{LC}}\omega t) \tag{7}$$

$$V_{dc}(t)=\frac{(12Vk-3V_1k-3V_2k)}{(4LC+12k^2)}-\frac{(3V_1k+3V_2k)}{4(LC-k^2)}\cos(2\omega t)+\frac{3(LV_1C-2LVC+LV_2C+2Vk^2+V_1k^2+V_2k^2)}{(LC-k^2)(6k^2+2LC)}\cos(\frac{\sqrt{(3k^2+LC)}}{\sqrt{LC}}\omega t) \tag{8}$$

$$|i_{-1}|=\sqrt{(\frac{V_{-1}C}{LC-k^2})^2+(\frac{V_{-1}C}{LC-k^2})^2(1-\frac{k^2}{2CL})^2}=(\frac{V_{-1}C}{LC-k^2})\sqrt{1+(1-\frac{k^2}{2CL})^2} \tag{9}$$

$$|V_{dch2}|=\frac{3V_{-1}k}{2(LC-k^2)} \tag{10}$$

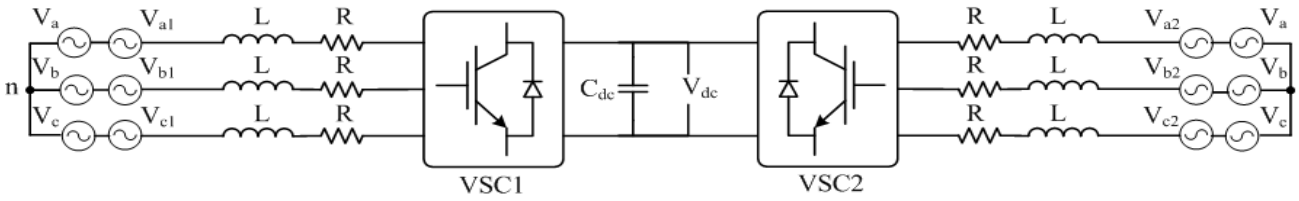

Fig. 2. Structure of active mobile substation.

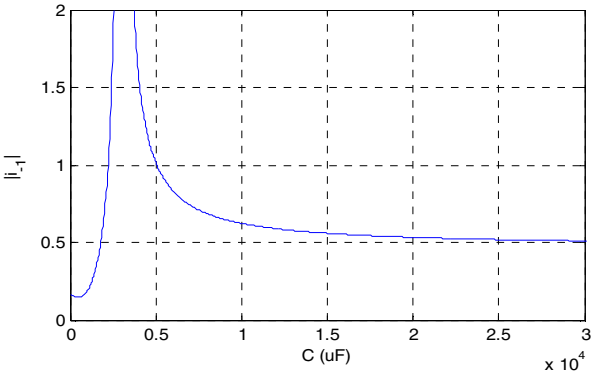

Fig. 3. The AMS negative sequence current component versus DC link capacitor (Theoretical Result)

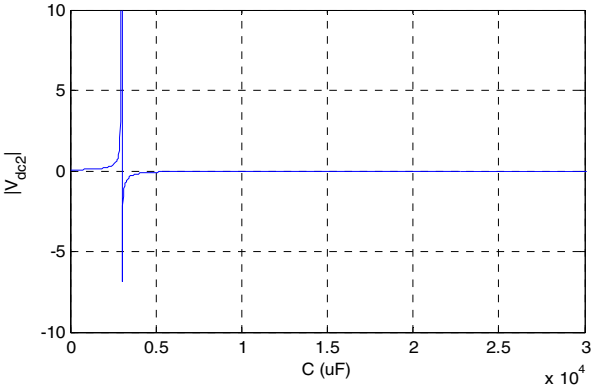

Fig. 4. The AMS second order harmonic component of dc bus voltage versus DC link capacitor (Theoretical Result)

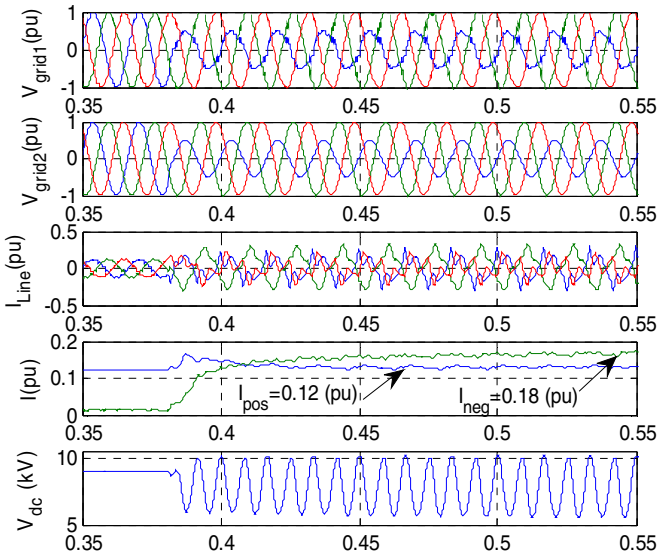

Fig. 5. Dynamic performance of angle-controlled AMS under unbalanced condition of 50% single-line voltage sag (C=1 mF).

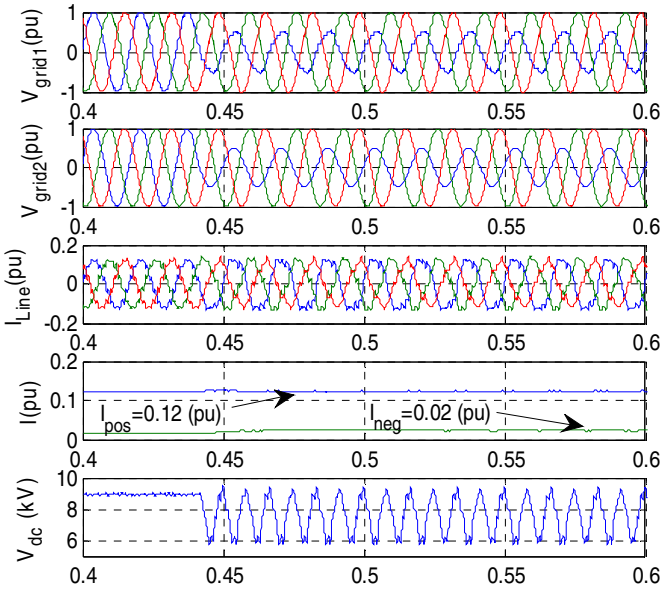

Fig. 6. Dynamic performance of angle-controlled AMS system under unbalanced condition of 50% single-line voltage sag (C=0.1 mF).

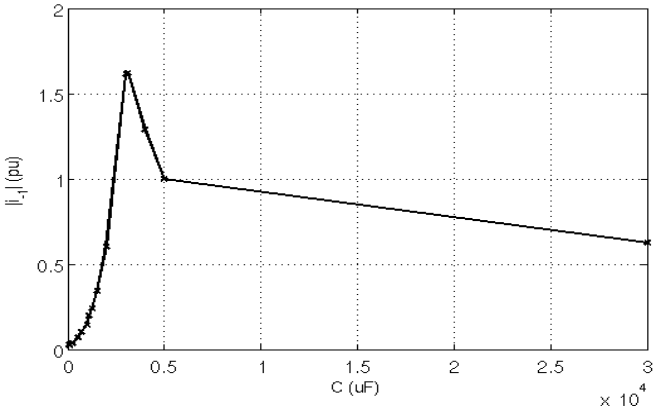

Fig. 7. The AMS negative sequence current component versus DC link capacitor (Simulation Result).

IV. Instantaneous Active Power Control of AMS

It was shown that component design criterion has some limitations on dynamic performance of the AMS under unbalanced conditions. This section proposes a supplementary control scheme suitable for high power mobile converters that improves the dynamic performance of the system under unbalanced operating conditions. The method is explained in the following.

Three-phase unbalanced input voltages and currents given by (11) can be expressed as a sum of positive and negative sequence components.

The instantaneous active power of the AMS can be written as (12). The average value and second harmonic components of the instantaneous active power can be defined as (13) and (14) respectively. The instantaneous active power is delivered to the dc link and determines the dc voltage level, and if it varies with time, the dc-link voltage fluctuates. Therefore, in order to keep constant dc level, $P_{ac}(t)$ should be nullified. Eqs. (15), (16), and (17) are not necessary but enough to eliminate $P_{ac}(t)$. The positive sequence current component can be found as (18) by substituting (15)-(17) into (13). As noted from (15)-(18), the positive and negative sequence components of input voltages should be computed in abc frame to obtain the reference values of positive and negative sequence components of input current, and switching angles are determined based on the reference input current. The obtained set of switching functions makes the instantaneous active power constant without any oscillating terms, and it maintains a robust dc link voltage under unbalanced operating conditions. The control structure of AMS based on the proposed method is shown in Fig. 8.

$$\begin{aligned} v_a &= V_{pk}^p \cos(\omega t+\theta_v^p)+V_{pk}^n \cos(\omega t+\theta_v^n) \\ v_b &= V_{pk}^p \cos(\omega t+\theta_v^p-\frac{2\pi}{3})+V_{pk}^n \cos(\omega t+\theta_v^n+\frac{2\pi}{3}) \\ v_c &= V_{pk}^p \cos(\omega t+\theta_v^p+\frac{2\pi}{3})+V_{pk}^n \cos(\omega t+\theta_v^n-\frac{2\pi}{3}) \end{aligned} \qquad \begin{aligned} i_a &= I_{pk}^p \cos(\omega t+\theta_i^p)+I_{pk}^n \cos(\omega t+\theta_i^n) \\ i_b &= I_{pk}^p \cos(\omega t+\theta_i^p-\frac{2\pi}{3})+I_{pk}^n \cos(\omega t+\theta_i^n+\frac{2\pi}{3}) \\ i_c &= I_{pk}^p \cos(\omega t+\theta_i^p+\frac{2\pi}{3})+I_{pk}^n \cos(\omega t+\theta_i^n-\frac{2\pi}{3}) \end{aligned} \tag{11}$$

$$P(t)=v_a i_a+v_b i_b+v_c i_c=\frac{3}{2}\begin{bmatrix} V_{pk}^p I_{pk}^p \cos(\theta_v^p-\theta_i^p)+V_{pk}^p I_{pk}^n \cos(2\omega t+\theta_v^p+\theta_i^n)+ \\ V_{pk}^n I_{pk}^p \cos(2\omega t+\theta_v^n+\theta_i^p)+V_{pk}^n I_{pk}^n \cos(\theta_v^n-\theta_i^n) \end{bmatrix} \tag{12}$$

$$P_{dc}=\frac{3}{2}\left[V_{pk}^p I_{pk}^p \cos(\theta_v^p-\theta_i^p)+V_{pk}^n I_{pk}^n \cos(\theta_v^n-\theta_i^n)\right] \tag{13}$$

$$P_{ac}(t)=\frac{3}{2}\left[V_{pk}^p I_{pk}^n \cos(2\omega t+\theta_v^p+\theta_i^n)+V_{pk}^n I_{pk}^p \cos(2\omega t+\theta_v^n+\theta_i^p)\right]=0 \tag{14}$$

$$V_{pk}^p I_{pk}^n = V_{pk}^n I_{pk}^p \Rightarrow \frac{I_{pk}^n}{I_{pk}^p}=\frac{V_{pk}^n}{V_{pk}^p} \Rightarrow I_{pk}^n=\frac{V_{pk}^n}{V_{pk}^p}\times I_{pk}^p \tag{15}$$

$$\pi+\theta_v^p+\theta_i^n=\theta_v^n+\theta_i^p \Rightarrow \theta_i^n=\theta_v^n-\pi \tag{16}$$

$$\theta_i^p=\theta_v^p \tag{17}$$

$$P_{dc}=\frac{3}{2}\left[V_{pk}^p I_{pk}^p-V_{pk}^n I_{pk}^n\right]=\frac{3}{2}\left[V_{pk}^p I_{pk}^p-(V_{pk}^n)^2\frac{I_{pk}^p}{V_{pk}^p}\right] \Rightarrow I_{pk}^p=\frac{P_{dc}}{\frac{3}{2}\left[V_{pk}^p-\frac{(V_{pk}^n)^2}{V_{pk}^p}\right]} \tag{18}$$

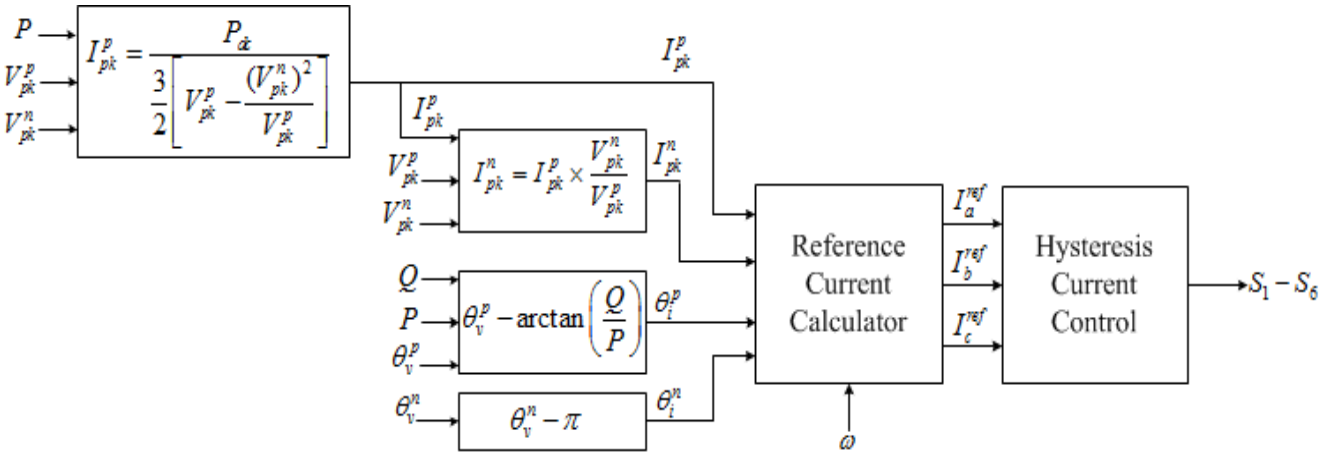

Fig. 8. Power flow based inverter control structure of AMS based on instantaneous active power flow control.

The AMS system parameters are tabulated in Table I. The dynamic performance of the AMS system under single line to ground (SLG) fault in the rectifier side (dc voltage controller converter) is presented in Fig. 9 when the reference value of active power is not varied during fault. When AC fault happens, the reference power can also be modified to very small value such as 50% of the rated power, and the negative sequence controller can be applied to reduce the active power fluctuation. Fig. 10 presents the dynamic performance of the AMS system under SLG fault when the reference value of active power is also reduced to %50 of rated power during fault.

Table I. AMS System Parameters

Base Power	S	9 MVA
Line-to-line peak voltage	E	4.5 kV
Line frequency (grid)	f	60 Hz
Input voltage phase	θ_s	5.74°
DC link voltage	V_{DC}	9 kV
DC link capacitance	C_{DC}	10 (mF)

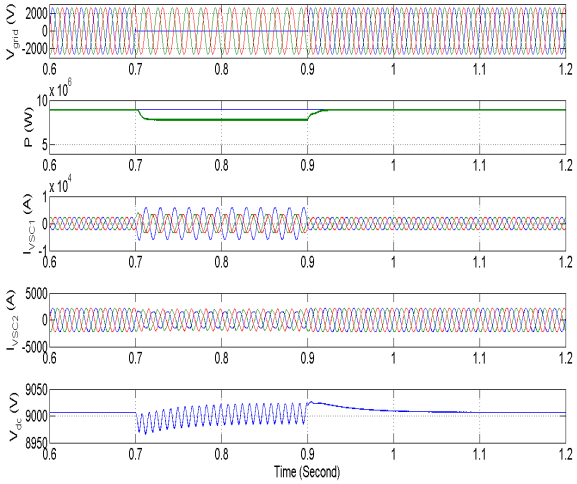

Fig. 9. Dynamic performance of the AMS system under SLG fault in the dc link voltage controller side with instantaneous active power controller (%100 power transfer during fault)

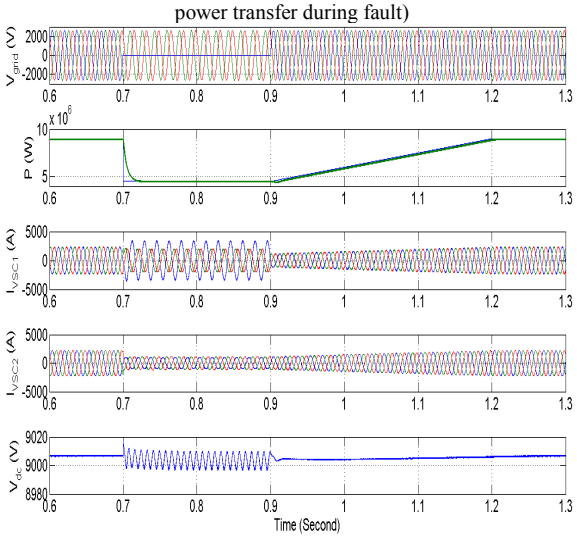

Fig. 10. Dynamic performance of the AMS system under SLG fault in the dc link voltage controller side with instantaneous active power controller (%50 power transfer during fault)

The supervisory control scheme should be designed to determine the control strategy under fault based on the negative sequence voltage component. The overall sketch of the supervisory control is presented in Fig. 11. The dynamic performance of the angle-controlled AMS system with 0.1mF DC link capacitors under 10% voltage drop in phase-A is shown in Fig. 12. As can be seen, the performance of angle-controlled AMS with appropriate component design under 10% voltage sag is acceptable. However, under 50% voltage sag in phase A, the supervisory control switches the control scheme from angle control method to the proposed instantaneous active power method, and the results are presented in Fig. 13. From Fig. 13, it can be observed that three phase input currents are in phase with the input voltages. The stiffness of dc bus voltage is evident in Fig. 13. Fig. 14 illustrates the positive and negative sequence components of three phase unbalanced voltages and currents. As can be seen, using the proposed control scheme leads a better dynamic performance compared to the case with just component design albeit with losing efficiency temporarily during significant system disturbances.

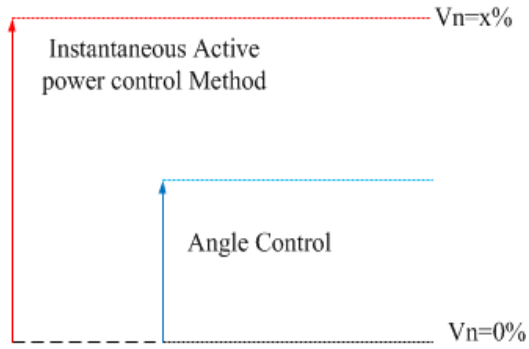

Fig. 11. The rough sketch of supervisory control for AMS operation based on the negative sequence voltage component (Vn).

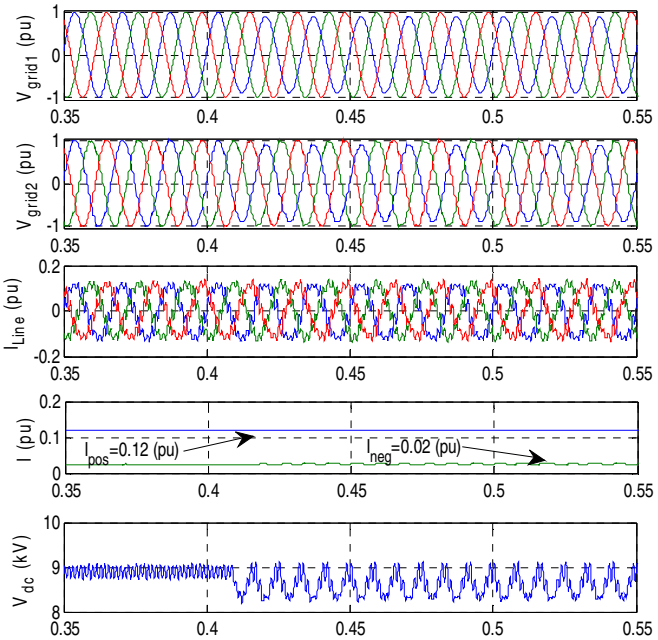

Fig. 12. Dynamic performance of the angle-controlled AMS system under an unbalanced condition of 10% single-line voltage sag.

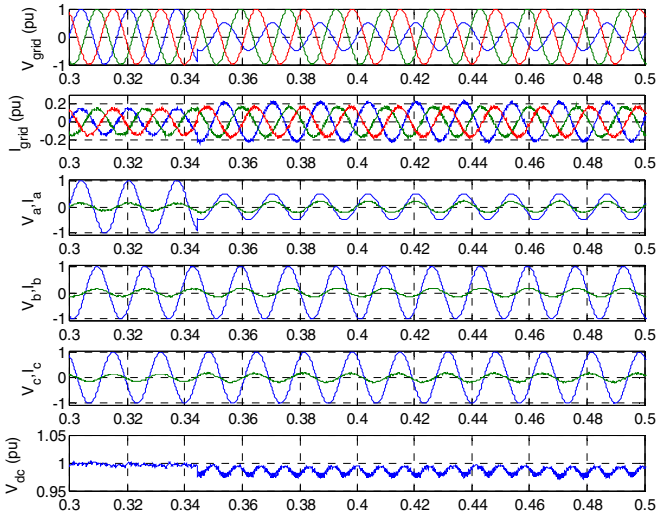

Fig. 13. Dynamic performance of the AMS under an unbalanced condition of 50% single-line voltage sag with the proposed method.

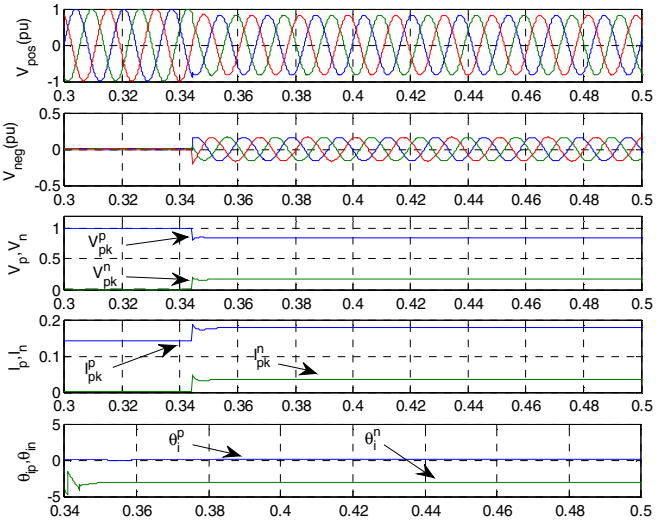

Fig. 14. Positive and negative sequence components of voltage and currents.

V. The AMS Experimental Test Bed

The AMS experimental test bed is shown in Fig. 15. The specifications of the experimental testbed can be summarized in Table. II. OZTEK controller is used to implement different control methods.

Dynamics of reactive power in the rectifier side of AMS based on angle control method is shown in Fig. 16 under normal operating conditions. Fig. 17 also shows dynamics of three phase ac current for this case scenario.

The unbalanced three-phase input voltages and the extracted voltage angle is shown in Fig. 18. As can be seen, there is 50% voltage sag in phase-a. The dc bus voltage and three phase ac current based on angle control method are shown in Figs. 19, and 20 respectively.

Fig. 21 shows dc bus voltage based on instantaneous active power method under unbalanced operating conditions. The stiffness of dc bus voltage is evident in Fig. 21. As can be seen, the proposed control method makes the instantaneous active power constant without any oscillating terms, and it maintains a robust dc link voltage under unbalanced operating condition. Three-phase ac current is also illustrated in Fig. 22. Fig. 23~Fig.25 also show the reference and measured value of three phase ac current based on instantaneous active power control method under unbalanced operating conditions.

Table II. Specifications of AMS Hardware prototype

Line-to-line peak voltage	E	208 V
Line frequency (grid)	f	60 Hz
sending-end Leakage inductance	L_s	5 (mH)
receiving-end Leakage inductance	L_r	5 (mH)
Switching frequency	f_{sw}	10 (kHz)
Converter Transformer	S_c	15 (kVA)
DC link capacitance	C_{DC}	2.5 (mF)

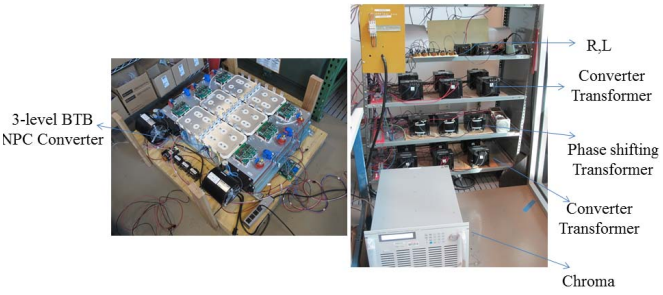

Fig. 15. Experimental test-bed for Active Mobile Substation based on 3-level NPC converter

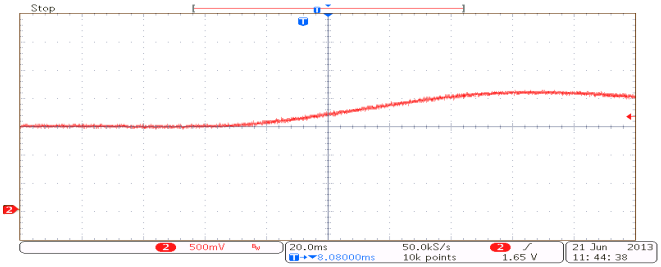

Fig. 16. Dynamics of reactive power when reactive power has a step change from 0 pu to 1.0 pu under normal operating condition (Angle control)

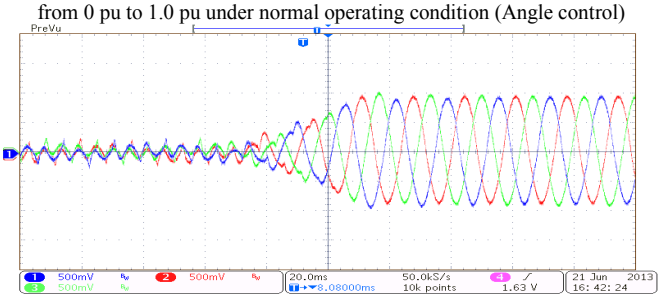

Fig. 17. Converter current when reactive power has a step change from 0 pu to 1.0 pu under normal operating condition (Angle Control)

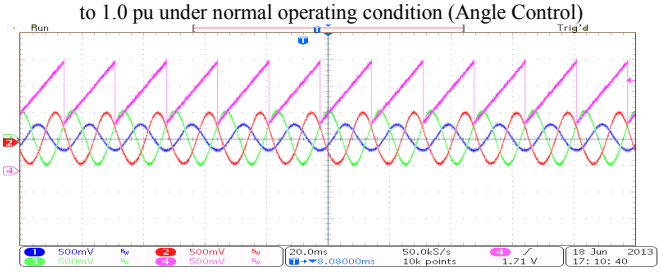

Fig. 18. Unbalanced three-phase input voltages and extracted voltage angle

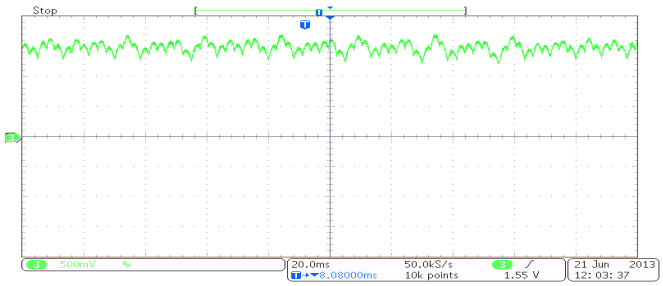

Fig. 19. DC bus voltage under unbalanced operating conditions (Angle control method)

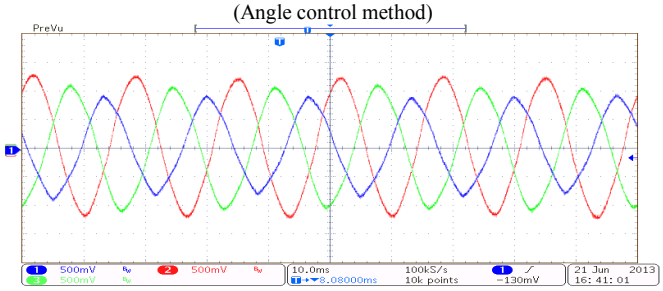

Fig. 20. Dynamics of three phase ac current under unbalanced operating conditions (Angle control method)

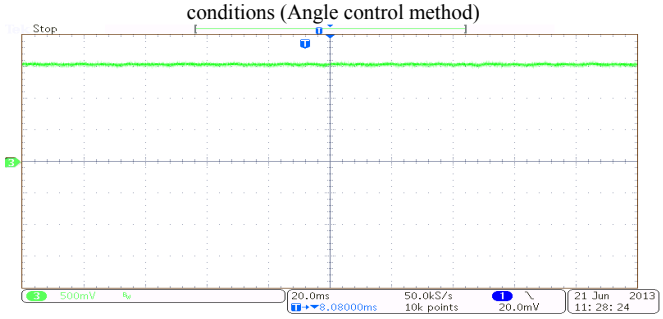

Fig. 21. DC bus voltage under unbalanced operating conditions (instantaneous active power control method)

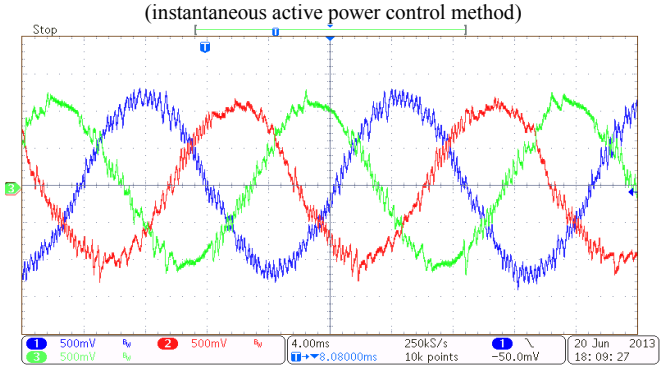

Fig. 22. Three phase ac current under unbalanced operating conditions (instantaneous active power control

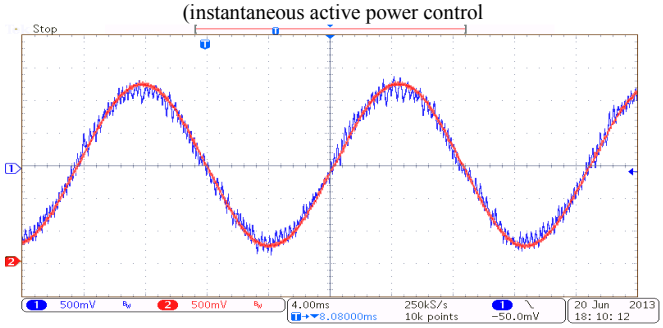

Fig. 23. The reference and measured value of phase-a ac current

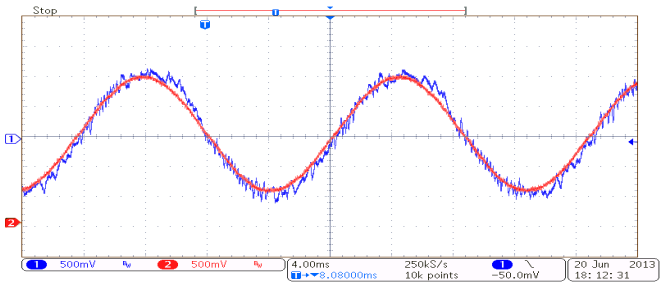

Fig. 24. The reference and measured value of phase-b ac current

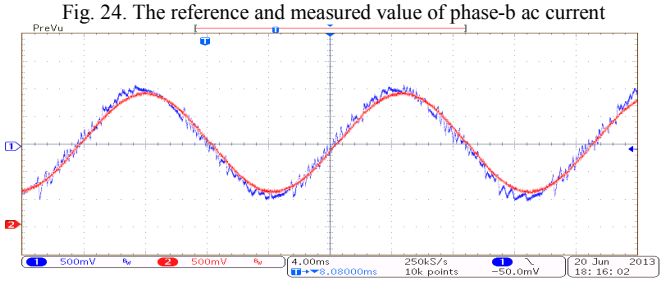

Fig. 25. The reference and measured value of phase-c ac current

VI. Conclusion

The concept of AMS as a viable utility asset is motivated by the fact that it can provide "flexible" control across existing utility power transformers with fractionally rated converter system; as well as provide lifetime extension of aging power transformers. In this paper, dynamic performance of AMS under unbalanced operating condition is examined. Results show that the negative sequence current is highly dependent on the DC capacitor value, and the capacitor value must be chosen appropriately such that 120 Hz oscillations in the DC link can be tolerated under unbalanced conditions. A control scheme based on instantaneous active power control method is also proposed to make dc bus voltage constant. A supervisory control is also used to determine the switching strategy between angle control method and proposed control method under fault operating conditions. Experimental results are also shown to verify the proposed control structure of AMS under unbalanced operating conditions.

Acknowledgment

This work made use of ERC shared facilities supported by the National Science Foundation under Award Number EEC-08212121.

References

[1] www.abb.com

[2] B. Parkhideh, N. Yousefpoor, S. Babaei and S. Bhattacharya, "Design considerations in development of active mobile substations," *In Proc. ECCE'12*, 2012.

[3] B. Parkhideh, N. Yousefpoor, B. Fardanesh and S. Bhattacharya, "Vector Analysis and Performance Evaluation of Modular Transformer Converter (MTC) Based Convertible Static Transmission Controller," *IEEE PES General Meeting, 2012*.

[4] C. Schauder, and H. Mehta., "Vector analysis and control of advanced static VAR compensators," *IEE Proc. -C*, July 1993.

[5] B. Parkhideh, and S. Bhattacharya, "Active power transfer capability of shunt family of FACTS devices base on angle control," *IEEE ECCE'09*.